Understanding the global structure of two-level quantum systems with relaxation: Vector fields organized through the magic plane and the steady-state ellipsoid

M. Lapert,[1] E. Assémat,[2] S. J. Glaser,[1] and D. Sugny[2,*]

[1]*Department of Chemistry, Technische Universität München, Lichtenbergstrasse 4, D-85747 Garching, Germany*

[2]*Laboratoire Interdisciplinaire Carnot de Bourgogne (ICB), UMR 6303 CNRS-Université de Bourgogne, 9 Av. A. Savary, BP 47 870, F-21078 Dijon Cedex, France*

(Received 3 June 2013; published 6 September 2013)

The understanding of the dynamics of a two-level quantum system with relaxation is one of the fundamental questions of quantum mechanics. We describe geometrically the structure of this system by introducing different vector fields, which give insight into the global dynamics of the system. The vector fields are organized through two basic geometric objects, the magic plane and the steady-state ellipsoid. We show how these latter help analyzing the time-optimal control of two-level dissipative quantum systems.

DOI: 10.1103/PhysRevA.88.033407 PACS number(s): 32.80.Qk, 37.10.Vz, 78.20.Bh

I. INTRODUCTION

The theoretical analysis of complex dynamical systems can be approached from two complementary points of view. The first one is based on numerical computations, the goal being mainly to simulate systems of growing complexity close to experimental conditions. The second option consists in understanding the qualitative structures of the dynamics via a geometric analysis of the system. These two theoretical techniques of analysis are, of course, not disconnected, and a precise understanding of the geometrical properties of the system can explain quantitative results of numerical simulations. It is this second geometric aspect which will be at the core of this work in order to analyze the dynamics of two-level quantum systems with relaxation. The description of the dynamics of two-level systems has always been one of the fundamental questions of quantum mechanics [1]. Recently, this subject has even attracted more attention because of the ideas of quantum computing [2]. In many physical applications, it can be sufficient to take into account only two of the energy eigenstates of the system, for example, those in resonance with the frequency of the control field [3,4]. The coherent quantum effects that can be observed in such systems are now well known in different fields extending from atomic and molecular physics [5] to nuclear magnetic resonance [6] and solid state physics. However, in order to deal with more realistic experimental conditions, it is crucial to account for environmental effects [7–14]. For instance, in quantum computing, a fundamental requirement is the preservation of the coherence in the presence of relaxation due to the interaction with the environment [2,15–17]. Theoretically, if one lacks a detailed microscopic description of the environment, the interaction of the quantum system with its surroundings can often be described by phenomenological relaxation processes. A general description of the effective dynamics of open quantum systems was given simultaneously by Lindblad [18] and Gorini *et al.* [19]. These equations have been established to ensure that the state of the system remains physically valid along the dynamics. In this rigorous mathematical framework, one crucial question is the analysis of the corresponding dynamics, in particular, for the simplest system, the two-state one. In this case, the dynamics, which is governed by the Bloch equation, is characterized by two relaxation times T_1 and T_2. Generally, the first step for studying such a dynamics consists in computing analytically the solutions of the Bloch equations through various approximations or particular cases (see [6,9,20–23] and references therein to cite a few). However, the explicit formulas of the corresponding trajectories are not very helpful and give only little insight into the main features of the dynamics. This analysis turns out to be relatively simple if one introduces some geometrical objects, which lead to a global overview of the dynamics.

The purpose of the present paper is to study from a geometric perspective the dynamics of two-level quantum systems in the presence of relaxation. This investigation is valid in the unbounded case. When the control field is bounded, the analysis is more involved mathematically and requires advanced tools of optimal control theory, such as the Pontryagin maximum principle [24–27]. As opposite to these recent results, this paper is accessible to a broad audience without a solid background in optimal control techniques. In this respect, this work can also be viewed as a pedagogical introduction which can help the interest the reader to enter into a more mathematical literature [25,26].

The paper is organized as follows. Starting from the Bloch equation in presence of relaxation, we introduce a general description of the dynamics in terms of vector fields in Sec. II. In Sec. III, we show that these vector fields are organized through two different geometric objects, the magic plane and the steady-state ellipsoid. We discuss the role of these two geometric structures in Sec. IV. A conclusion and prospective views are given in Sec. V.

II. THE BLOCH EQUATION IN TERMS OF VECTOR FIELDS

We consider a two-state quantum system in the presence of relaxation whose dynamics can be described by the following Bloch equation:

$$\begin{aligned} \dot{x} &= -\frac{x}{T_2} + u_y z, \quad \dot{y} = -\frac{y}{T_2} - u_x z, \\ \dot{z} &= \frac{(1-z)}{T_1} + u_x y - u_y x, \end{aligned} \tag{1}$$

*dominique.sugny@u-bourgogne.fr

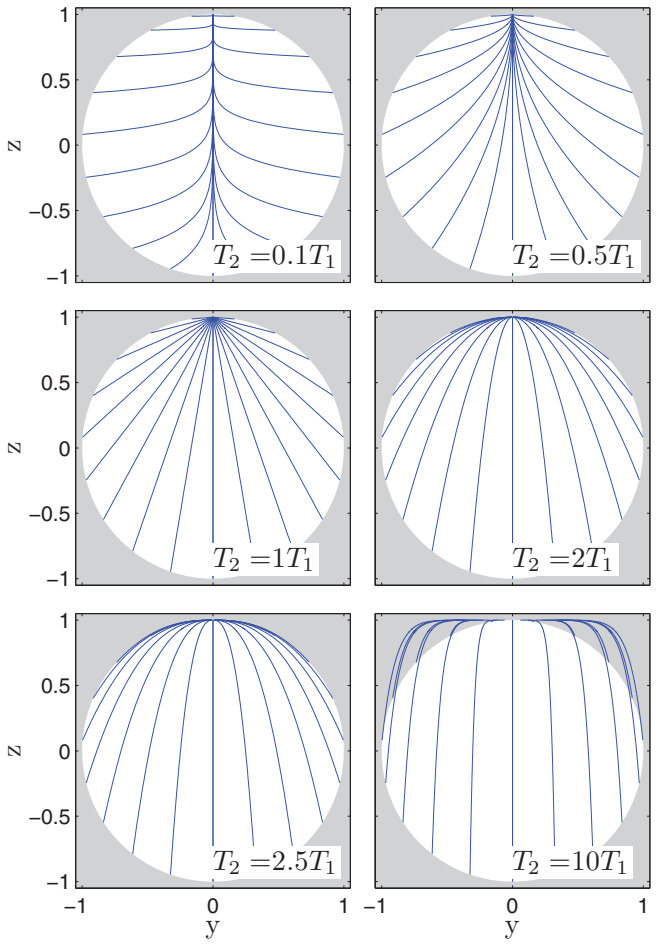

FIG. 1. (Color online) Free dynamics for different T_1/T_2 ratios. The starting points of the trajectories belong to the Bloch sphere of radius 1.

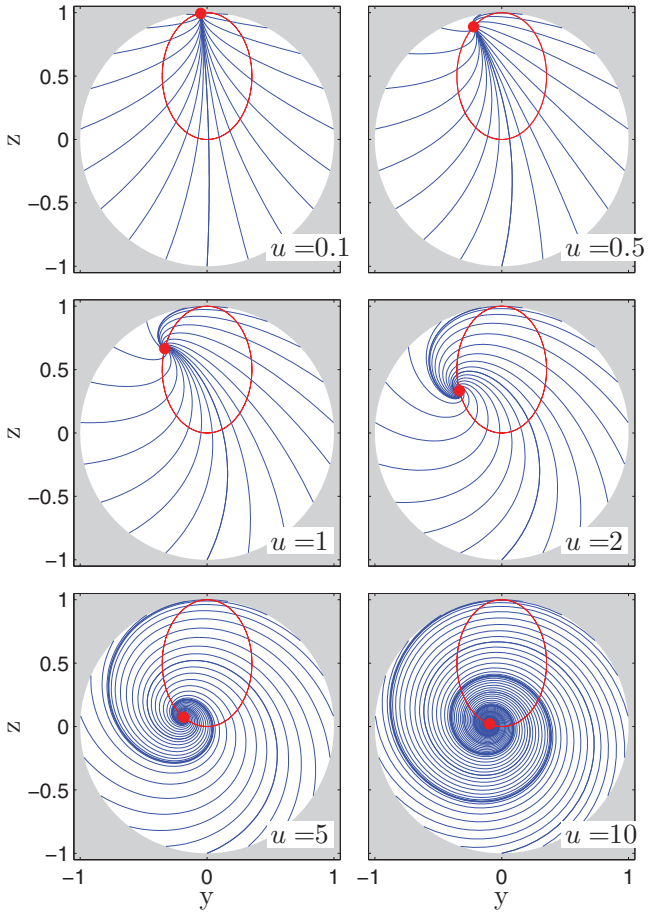

FIG. 2. (Color online) Trajectories of the quantum system in the (y,z) plane submitted to a constant control field u_x. Each panel corresponds to a different value of u_x. The relaxation rates are taken to be $T_1 = 1$ and $T_2 = 0.5$. The initial points belong to the Bloch sphere. The second vector field u_y is assumed to be zero. The limit points of the dynamics are represented by a red (dark gray) ellipse curve. The transition from a pseudoperiodic to an aperiodic regime occurs for $u_x = 0.5$.

where u_x and u_y are the two components of the control field, which is assumed to be on resonance with the frequency of the quantum system [6]. The off-resonance case is not treated here, but could be made with the same tools. The Bloch vector $\vec{X} = (x,y,z)$ describes the position of the system at a given time in the Bloch ball, defined by $x^2 + y^2 + z^2 \leqslant 1$. To simplify the discussion, we consider here a specific case of the Lindblad equation, in which the thermal equilibrium point is the north pole of the Bloch sphere. The same analysis can be done along the same lines in other configurations. The parameters T_1 and T_2 account for the relaxation effects along the longitudinal and transverse directions, respectively. The two relaxation rates satisfy the relations $0 \leqslant T_2 \leqslant 2T_1$ to ensure that $|\vec{X}| \leqslant 1$ at any time [18,19]. This feature is illustrated in Fig. 1, which displays a series of free dynamics in the (y,z) plane for different T_1/T_2 ratios. If $T_2 > 2T_1$, note that some trajectories go out of the Bloch ball, which is not possible in the general case [28–30]. For nonzero but constant control fields, the evolution of the quantum system can be completely different, as shown in Fig. 2. A qualitative change of the trajectories is observed according to the value of the field. A direct analytical computation shows a transition from a pseudoperiodic solution to an aperiodic one when the value of u_x decreases. Note also that the state of the system tends asymptotically towards a point of an ellipse curve represented in Fig. 2. This ellipse is the two-dimensional trace of a three-dimensional ellipsoid when the two control fields are considered (see Fig. 6 for a representation). Every point of the ellipsoid can be reached by a trajectory of the system, the north pole of the Bloch sphere corresponding to the limit point of the free dynamics. Since this ellipsoid is well known in nuclear magnetic resonance as the location of the steady state for continuous wave irradiation [6], we refer to it as the steady-state ellipsoid.

The results of Figs. 1 and 2 constitute a first step in the analysis of this dynamical system. However, this approach provides a large amount of data, which cannot be easily interpreted. A completely different point of view emerges if this problem is approached from a geometric perspective, leading thus to a global description of the dynamics. The first elementary object to introduce is the notion of vector field, i.e., the assignment of a vector to each point of the Bloch ball. This mathematical tool will serve as a building block

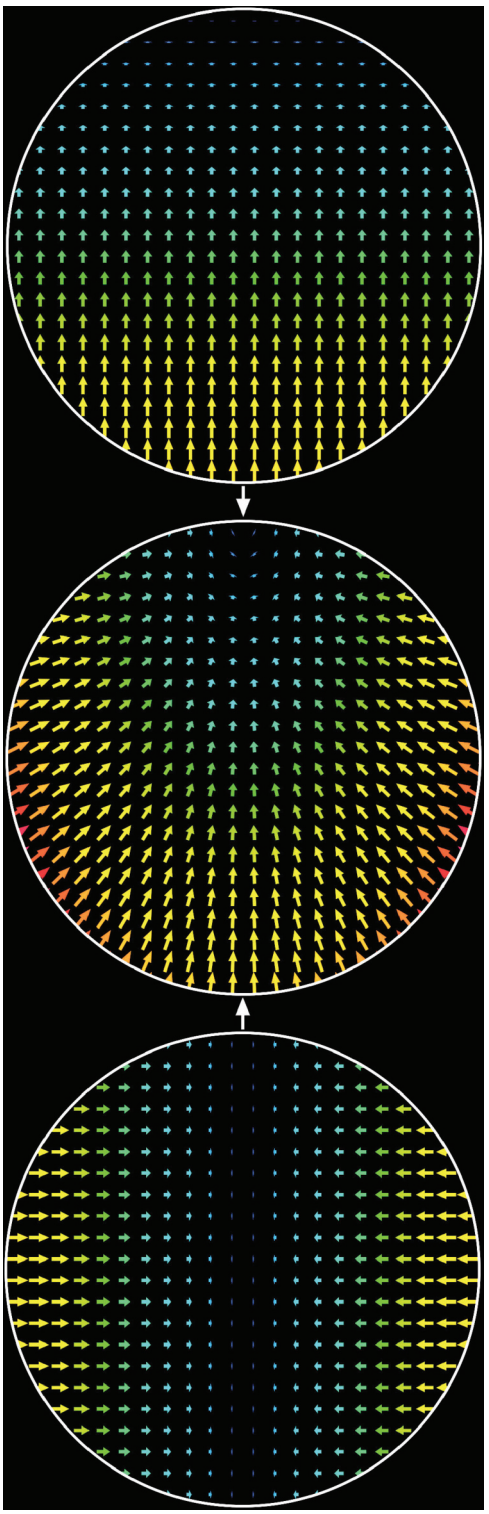

FIG. 3. (Color online) Global representation in the (y,z) plane of the vector fields $\vec{R}_1$ (top panel), $\vec{R}_2$ (bottom panel), and $\vec{R}$ (middle panel). The small arrows depict the corresponding fields at discrete points. The color map encodes the length of the vectors. The parameters are taken to be $T_1 = 1$ and $T_2 = 0.5$.

for the more advanced geometric concepts treated in the next sections. According to the parametrization used to describe the dynamical system, different vector fields can be defined. In the simplest case of Cartesian coordinates, the system can be rewritten in a vectorial form as follows:

$$\dot{\vec{X}} = \vec{R}(\vec{X}) + u_x \vec{P}_x(\vec{X}) + u_y \vec{P}_y(\vec{X}), \tag{2}$$

where $\vec{R}(\vec{X}) = (-x/T_2, -y/T_2, [1-z]/T_1)$, $\vec{P}_x(\vec{X}) = (0, -z, y)$, and $\vec{P}_y(\vec{X}) = (z, 0, -x)$ are three vector fields associated with the uncontrolled and controlled parts of the dynamics. The drift vector $\vec{R}$ can also be decomposed into a T_1 part and a T_2 part, denoted $\vec{R}_1(\vec{X}) = (0, 0, [1-z]/T_1)$ and $\vec{R}_2(\vec{X}) = (-x/T_2, -y/T_2, 0)$, respectively. The information encoded in the vector field can be globally represented by a set of small arrows whose length and direction show the magnitude and direction of the corresponding vector. This point is illustrated in Fig. 3 for the vector fields $\vec{R}_1$, $\vec{R}_2$, and $\vec{R}$. The definition of a vector field is invariant and does not depend on the choice of the parametrization. Introducing the spherical coordinates given by

$$x = r\cos\theta\cos\phi, \quad y = r\cos\theta\sin\phi, \quad z = r\sin\theta,$$

one obtains the following relation between the time derivatives:

$$\begin{aligned} \dot{r} &= \cos\theta\cos\phi\dot{x} + \cos\theta\sin\phi\dot{y} + \sin\theta\dot{z}, \\ r\dot{\theta} &= -\sin\theta\cos\phi\dot{x} - \sin\theta\sin\phi\dot{y} + \cos\theta\dot{z}, \\ r\cos\theta\dot{\phi} &= -\sin\phi\dot{x} + \cos\phi\dot{y}. \end{aligned}$$

Using Eq. (1), one arrives at

$$\begin{aligned} \dot{r} &= -\frac{r\cos^2\theta}{T_2} + \frac{\sin\theta}{T_1} - \frac{r\sin^2\theta}{T_1}, \\ \dot{\theta} &= \frac{\cos\theta}{T_1}\left(\frac{1}{r} - \sin\theta\right) + \frac{\cos\theta\sin\theta}{T_2} + u_x\sin\phi - u_y\cos\phi, \\ \dot{\phi} &= -\tan\theta(u_y\sin\phi + u_x\cos\phi). \end{aligned} \tag{3}$$

In this case, the Bloch vector $\vec{X}$ is of coordinates (r,θ,ϕ) and the components of the relaxation vector fields $\vec{R}_1$ and $\vec{R}_2$ are $(\sin\theta - r\sin^2\theta, \cos\theta[1/r - \sin\theta], 0)/T_1$ and $(-r\cos^2\theta, \cos\theta\sin\theta, 0)/T_2$, respectively. With these coordinates, the radial and orthoradial components of $\vec{R}$, denoted $\vec{R}_r$ and $\vec{R}_\theta$, can also be defined as vector fields. The decomposition of the vector field $\vec{R}$ into its radial part $\vec{R}_r$ and its circular part $\vec{R}_\theta$ is illustrated in Fig. 4. In the radial panel, we also observe in black the occurrence of the ellipse of Fig. 2, for which the modulus of $\vec{R}_r$ is zero (see below for details). Figure 5 shows the combination of the $\vec{R}$ and $\vec{P}_x$ vector fields, which leads to the full vector field during a constant pulse. To summarize this first section, we point out that all the information about the quantum dynamics is encoded in the different vector fields. This formulation of the dynamics will be fundamental in the following to interpret the dynamics in presence of relaxation.

III. GEOMETRIC STRUCTURES: STEADY-STATE ELLIPSOID AND MAGIC PLANE

A standard way to describe the differential system (2) is based on the computation of the invariant points $\vec{X}$ such that $\dot{\vec{X}} = 0$ for some arbitrary constant values of the fields u_x and u_y. This set of points can be mathematically determined from the relation

$$\vec{R} + u_0\vec{P}_x + u_1\vec{P}_y = \vec{0}, \tag{4}$$

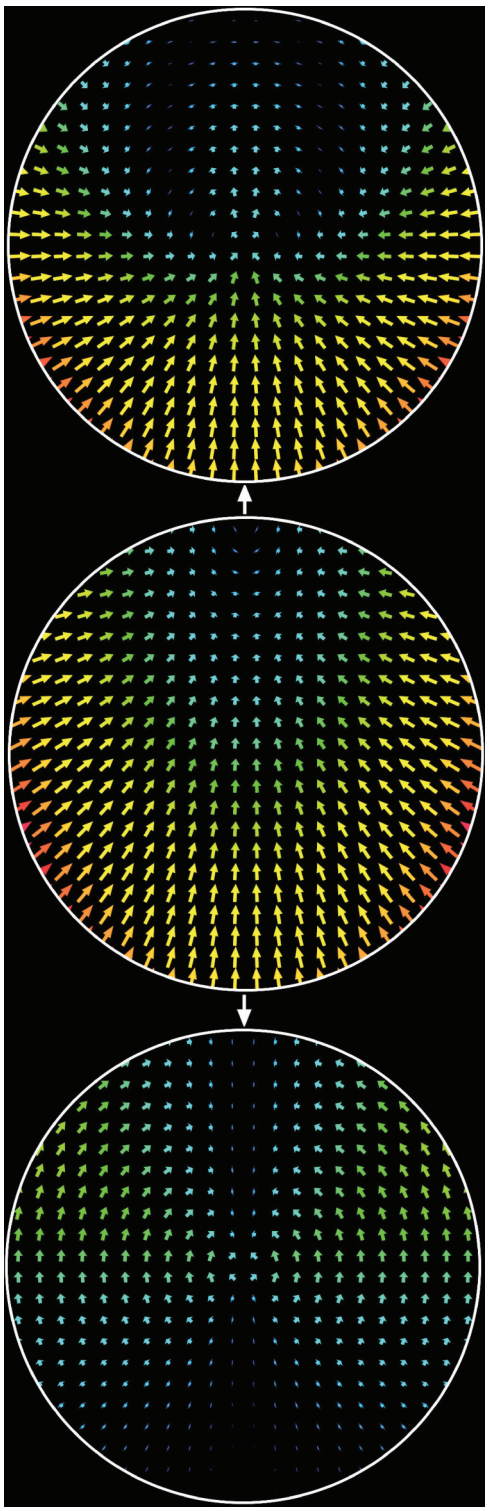

FIG. 4. (Color online) Same as Fig. 3 but for the spherical coordinates and the vector fields $\vec{R}_r$ (top panel: radial part), $\vec{R}_\theta$ (bottom panel: circular part), and $\vec{R}$ (middle panel). The amplitude of the field is $u_x = 2$.

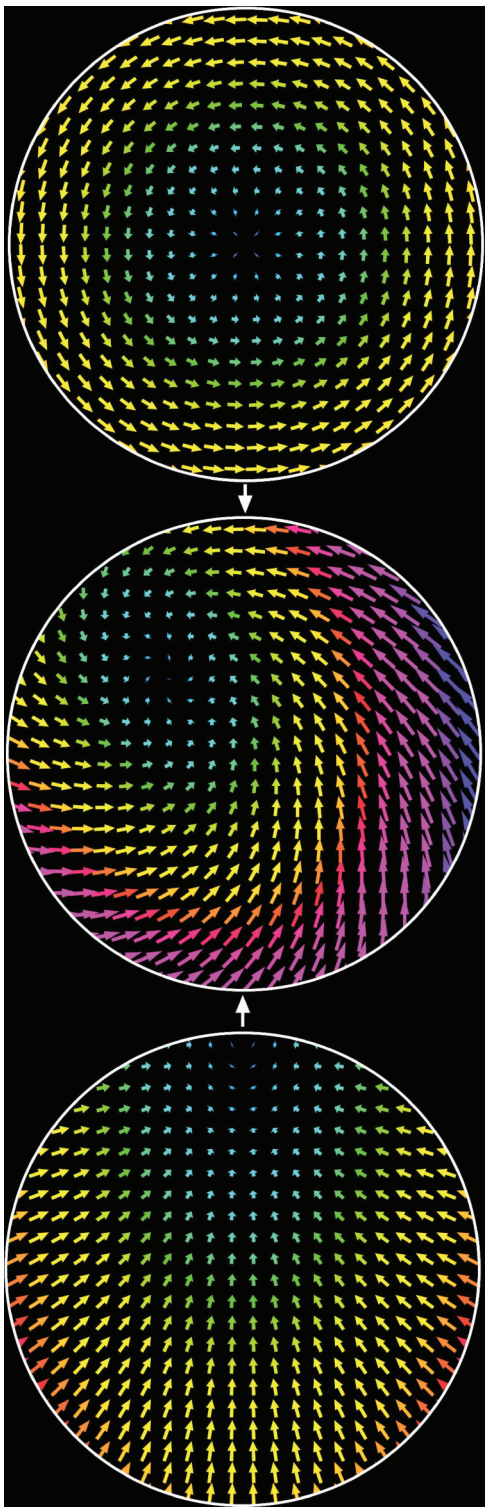

FIG. 5. (Color online) Same as Fig. 3 but for the vector fields $\vec{R}$ (bottom panel), $\vec{P}_x$ (top panel), and the sum $\vec{R} + u_x \vec{P}_x$ with $u_x = 2$ (middle panel).

where $u_x = u_0$ and $u_y = u_1$. In other words, this set, denoted $\mathcal{C}$, can be interpreted as the collinear locus of the vector fields $\vec{R}$, $\vec{P}_x$, and $\vec{P}_y$, i.e., as the set of points for which $\vec{R}$ belongs to the vectorial plane defined by the vectors $\vec{P}_x$ and $\vec{P}_y$. Using the vectorial product $\vec{P}_x \times \vec{P}_y$ of $\vec{P}_x$ and $\vec{P}_y$, of components (xz, yz, z^2), the collinear locus is obtained through the equation:

$$\vec{R} \cdot (\vec{P}_x \times \vec{P}_y) = 0, \tag{5}$$

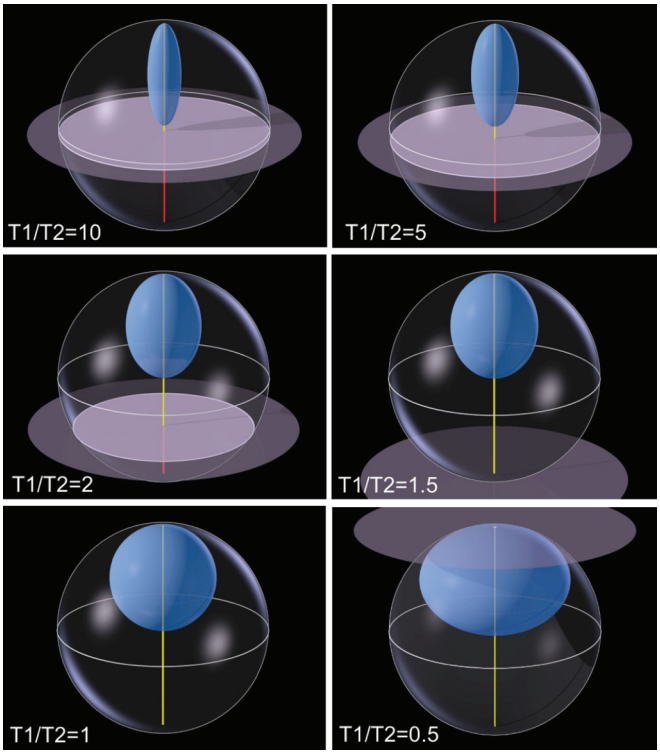

FIG. 6. (Color online) Plot of the steady-state ellipsoid in blue (dark gray) and of the magic plane in gray for different T_1/T_2 ratios (see the text for details). The Bloch sphere and the equator are only shown to guide the eye. The z axis is represented in yellow and in pink for the part above and below the magic plane, respectively.

which explicitly leads to

$$-\frac{x^2 z}{T_2} - \frac{y^2 z}{T_2} + \frac{(1-z)z^2}{T_1} = 0. \tag{6}$$

For $z \neq 0$, one gets a relation of the form

$$\frac{x^2+y^2}{T_2} + \frac{z^2}{T_1} - \frac{z}{T_1} = 0. \tag{7}$$

Equation (7) can be written as follows:

$$\frac{x^2+y^2}{T_2} + \frac{(z-1/2)^2}{T_1} = \frac{1}{4T_1}, \tag{8}$$

which corresponds to an ellipsoid of revolution. The only intersection point of the steady-state ellipsoid with the z axis is the center of the Bloch ball. Since this point trivially belongs to $\mathcal{C}$ [see Eq. (7)], one deduces that the collinear locus is exactly the ellipsoid. This geometric object is displayed in Fig. 6 for different values of T_1/T_2.

Another interesting characterization of this locus can be made by computing the time evolution of the radius $r = \sqrt{x^2+y^2+z^2}$. Its time derivative can be expressed as

$$\frac{1}{2}\frac{d}{dt}(r^2) = x\dot{x} + y\dot{y} + z\dot{z} = -\frac{x^2}{T_2} - \frac{y^2}{T_2} + \frac{z(1-z)}{T_1}, \tag{9}$$

which gives exactly the definition of $\mathcal{C}$ when this derivative is zero. We notice that this derivative does not depend on the control fields u_x and u_y since, physically, the fields cannot directly compensate for the effect of the relaxation [31]. The points inside the region delimited by the ellipsoid satisfy $\frac{d}{dt}(r^2) > 0$, while for the points outside $\frac{d}{dt}(r^2) < 0$. The surface $\mathcal{C}$ divides, therefore, the space (x,y,z) into a region where the modulus of the Bloch vector locally increases and a region where it locally decreases. On the boundary $\mathcal{C}$, the modulus is preserved. This point can be qualitatively understood by noting that the vector fields $\vec{P}_x$ and $\vec{P}_y$ are rotation vector fields which are orthoradial (i.e., normal to radial vectors) for each point $(x,y,z) \neq (0,0,0)$. The relaxation vector field $\vec{R}$ does not modify the modulus of $\vec{X}$ if its radial component vanishes, i.e., if $\vec{R}$ belongs to the vectorial plane defined by the vectors $\vec{P}_x$ and $\vec{P}_y$ (vectors with a zero radial component), which is the definition of the surface $\mathcal{C}$.

The inspection of the system (3) clearly shows that the control fields u_x and u_y can only change the orthoradial velocities $\dot{\theta}$ and $\dot{\phi}$ and not directly the radial one $\dot{r}$. The fields u_x and u_y move instantaneously the state of the system along any sphere belonging to the Bloch ball, i.e., along the θ and ϕ directions if no constraint on the intensity of the fields is used [24]. The remaining question is, therefore, to which extent the radial dynamics can be controlled. In this framework, the goal is to determine the points where the change of the radial coordinate, i.e., the radial velocity $\dot{r}$, is maximum, minimum, or zero [32]. As can be seen in Eq. (3), the derivative $\dot{r}$ only depends on the orthoradial direction θ, and not on the control fields. The radial dynamics cannot, therefore, be directly controlled, but only in a two-step process through the control of the angle θ.

For a given sphere of fixed radius r, the points of interest are given by the zeros of the derivative of $\dot{r}$ with respect to θ. Straightforward computations lead to

$$\frac{d\dot{r}}{d\theta} = \frac{2r\cos\theta\sin\theta}{T_2} + \frac{\cos\theta}{T_1} - \frac{2r\cos\theta\sin\theta}{T_1}, \tag{10}$$

which can be written in the original coordinates as follows:

$$\frac{d\dot{r}}{d\theta} = \frac{\sqrt{x^2+y^2}}{\sqrt{x^2+y^2+z^2}}\left(\frac{2z}{T_2} + \frac{1}{T_1} - \frac{2z}{T_1}\right). \tag{11}$$

The maximum or minimum variation of the radius r is given by the zeros of the derivative, $\frac{d\dot{r}}{d\theta} = 0$. The set of solutions is the union of a plane of equation

$$z = z_0 = \frac{T_2}{2(T_2 - T_1)},$$

that we denote the **magic plane** and of the z axis. This plane is represented in Fig. 6 for different T_1 and T_2 values. The magic plane intersects the Bloch ball if

$$\frac{T_2}{2|T_2 - T_1|} \leqslant 1. \tag{12}$$

In the case where $T_1 \geqslant T_2$, this leads to the condition $2T_1 \geqslant 3T_2$. Fixing the parameter T_1, the coordinate z_0 decreases from 0 to -1 for T_2 going from 0 to $T_2 = \frac{2}{3}T_1$. In the opposite case where $2T_1 \geqslant T_2 > T_1$, the only solution is $T_2 = 2T_1$, which corresponds to $z_0 = 1$. These results are summarized in Fig. 7.

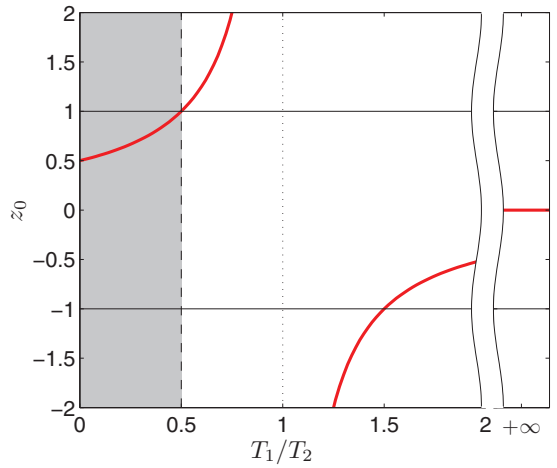

FIG. 7. (Color online) Position z_0 of the magic plane as a function of the ratio T_1/T_2 (red solid lines). The white zone represents the physically accessible region for which $-1 \leqslant z_0 \leqslant 1$ and $T_1/T_2 \geqslant 1/2$. The solid horizontal lines correspond to the limits of the Bloch ball.

The maximum or minimum character of the radial velocity is given by the second derivative of $\dot{r}$ with respect to the angle θ:

$$\frac{d^2\dot{r}}{d\theta^2} = \frac{1}{r}\left[2(\sqrt{x^2+y^2}-z^2)\left(\frac{1}{T_2}-\frac{1}{T_1}\right)-\frac{z}{T_1}\right]. \quad (13)$$

For the z axis ($x = y = 0$), it is straightforward to check that a maximum in absolute value is reached for $z_0 < z < 0$, i.e., for the points located between the magic plane and the steady-state ellipsoid. A minimum is obtained if $z < z_0 \leqslant 0$. If $z_0 > 0$, the points of the z axis outside the ellipsoid are also maxima. In this last case, since $\dot{r} < 0$, such points are associated with a maximum shrinkage of the value of the radius r. All the points of the magic plane for which $z = z_0$ also correspond to a maximum in absolute value of $\dot{r}$. The magic plane can, therefore, be viewed as a set of maximum shrinking directions of the radial coordinate. Finally, it can be shown that the the growth of r is maximum on the portion of the z axis for which $0 \leqslant z \leqslant 1$. A global description of $\dot{r}$ in the (y,z) plane is depicted in Fig. 8.

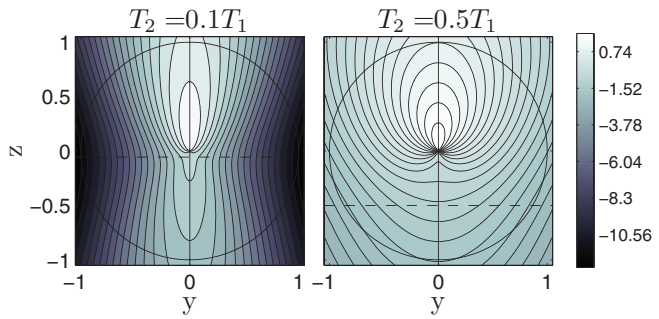

FIG. 8. (Color online) Contour plot of $\dot{r}$ in the (y,z) plane for two sets of (T_1,T_2) values. The dashed and solid lines represent, respectively, the projections of the magic plane and of the Bloch sphere.

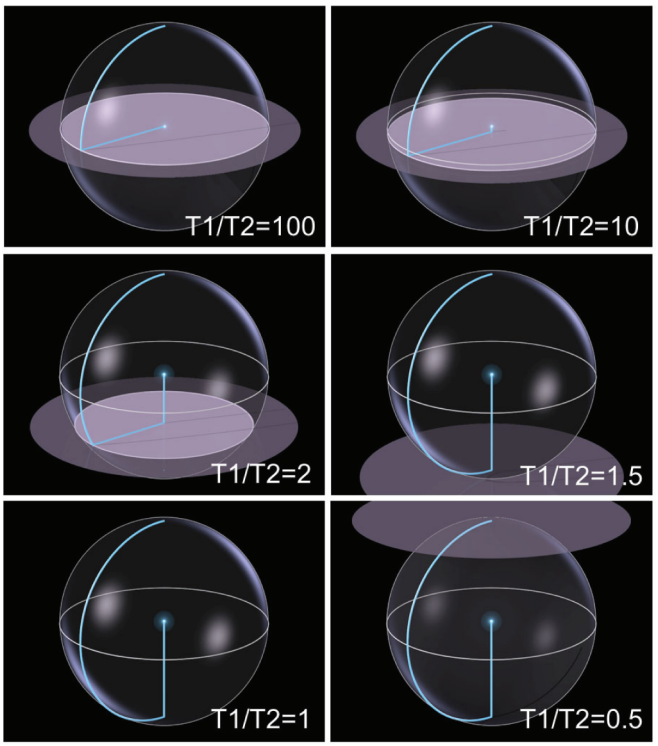

FIG. 9. (Color online) Optimal trajectories to reach in minimum time the center of the Bloch ball for different sets of $(T_1,\ T_2)$ parameters. The initial point of the dynamics is the north pole of the Bloch ball.

IV. APPLICATION TO THE TIME-OPTIMAL CONTROL OF A DISSIPATIVE TWO-LEVEL QUANTUM SYSTEM

We show in this section how to use the preceding geometric objects in order to determine the quickest way to connect two points of the Bloch ball. In the control terminology, this corresponds to solving a time-optimal control problem [24]. We recall that no bound is considered for the control field. The first step of this analysis consists in computing the constraints on the control fields to travel along the magic plane. To ensure that $z = z_0$ at any time, the following equation has to be fulfilled:

$$\dot{z} = 0 = \frac{(1-z_0)}{T_1} + u_x y - u_y x, \quad (14)$$

leading to a relation between u_x and u_y.

Figure 9 displays different optimal trajectories for reaching the center of the Bloch ball from the north pole. This constitutes a standard example of a control problem in nuclear magnetic resonance [24]. When $-1 < z_0 < 0$, the optimal solution is the concatenation of a circular arc to reach the magic plane, followed by a moving along this plane up to the z axis. The control field is then switched to zero to follow this line. As shown in Sec. III, the z axis between the magic plane and the ellipsoid maximizes the absolute value of the radial velocity and thus minimizes the time to reach the center of the Bloch ball. In the case where $z_0 < -1$ or $z_0 \geqslant 1$, the magic plane does not intersect the Bloch ball and only the z axis can be used from the south pole to the center of the Bloch ball. A particular case for which $z_0 \in (-1,0)$ is represented in Fig. 10.

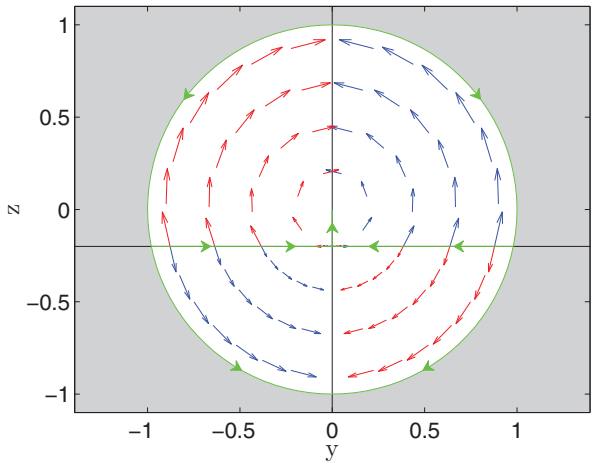

FIG. 10. (Color online) Optimal synthesis in the (y,z) plane in the case of an unbounded optimal control field. The initial state is the north pole of the Bloch ball. The blue (black) and red (dark gray) arrows represent the control vector field $u_x \vec{P}_x$ for positive and negative values of u_x, respectively. The green (light gray) lines display different examples of optimal trajectories, which can use the magic plane and the z axis. The ratio T_1/T_2 is taken to be 3/5, which gives $z_0 = -0.2$.

V. CONCLUSION

We have presented a geometric analysis of the dynamics of a two-level quantum system in presence of relaxation. The procedure is built from the introduction of particular vector fields which are organized around two fundamental geometric objects: the steady-state ellipsoid and the magic plane. By their simplicity and generality, the results of this work lead to important insights into the way to manipulate such systems. As such, they should be given the status of a fundamental textbook concept in quantum control. In this paper, only the unbounded case has been analyzed. The complete description of the bounded situation is far more involved than the one described here. This analysis requires advanced tools of geometric optimal control theory, but also in this case the steady-state ellipsoid and the magic plane play a fundamental role. In particular, the magic plane is defined in the control terminology as the singular locus, i.e., the manifold where the intensity of the optimal control field is lower than the prescribed bound. We refer the reader to the works [24,33,34] for a more detailed background on this approach.

ACKNOWLEDGMENTS

S.J.G. acknowledges support from the DFG (GI 203/7-1), SFB 631, and the Fonds der Chemischen Industrie. M.L. acknowledges support from Alexander von Humboldt Stiftung. D.S. and S.J.G. acknowledge support from the French-Bavarian project and from the PICS program of the CNRS. E.A. is supported by the Koshland Center for Basic Research. Financial support from the QUAINT coordination action (EC FET-Open) is gratefully acknowledged.

[1] A. Messiah, *Quantum Mechanics* (Dunod, Paris, 1995).
[2] M. A. Nielsen and I. L. Chuang, *Quantum Computation and Quantum Information* (Cambridge University Press, Cambridge, UK, 2000).
[3] S. Rice and M. Zhao, *Optimal Control of Quantum Dynamics* (Wiley, New York, 2000).
[4] M. Shapiro and P. Brume, *Principles of Quantum Control of Molecular Processes* (Wiley, New York, 2003).
[5] C. Brif, R. Chakrabarti, and H. Rabitz, New J. Phys. **12**, 075008 (2010).
[6] M. H. Levitt, *Spin Dynamics: Basics of Nuclear Magnetic Resonance* (John Wiley and Sons, Hoboken, NJ, 2008); R. R. Ernst, *Principles of Nuclear Magnetic Resonance in One and Two Dimensions*, International Series of Monographs on Chemistry (Oxford University Press, Oxford, UK, 1990).
[7] H.-P. Breuer and F. Petruccione, *The Theory of Open Quantum Systems* (Oxford University Press, Oxford, UK, 2002).
[8] B. B. Laird, J. Budimir, and J. L. Skinner, J. Chem. Phys. **94**, 4391 (1991).
[9] D. Traficante, *Encyclopedia of Nuclear Magnetic Resonance* (John Wiley and Sons, Chichester, 1996), p. 3988.
[10] E. Geva, R. Kosloff, and J. L. Skinner, J. Chem. Phys. **102**, 8541 (1995).
[11] M. Lapert, Y. Zhang, M. Janich, S. J. Glaser, and D. Sugny, Sci. Rep. **2**, 589 (2012).
[12] R. Roloff, M. Wenin, and W. Pötz, J. Comput. Theor. Nanosci. **6**, 1837 (2009).
[13] J.-S. Lee, R. R. Regatte, and A. Jerschow, Chem. Phys. Lett. **494**, 331 (2010).
[14] T. Viellard, F. Chaussard, D. Sugny, B. Lavorel, and O. Faucher, J. Raman Spec. **39**, 694 (2008).
[15] V. Mukheizee, A. Carlini, A. Mari, T. Caneva, S. Montangero, T. Calarco, R. Fazio, and V. Giovannetti (unpublished).
[16] D. Stefanatos, N. Khaneja, and S. J. Glaser, Phys. Rev. A **69**, 022319 (2004).
[17] D. Stefanatos, S. J. Glaser, and N. Khaneja, Phys. Rev. A **72**, 062320 (2005).
[18] G. Lindblad, Commun. Math. Phys. **40**, 147 (1975).
[19] V. Gorini, A. Kossakowski, and E. C. G. Sudarshan, J. Math. Phys. **17**, 821 (1976).
[20] A. D. Bain, C. K. Anand, and Z. Nie, J. Magn. Reson. **206**, 227 (2010).
[21] G. A. Morris and P. B. Chilvers, J. Magn. Reson., Ser. A **107**, 236 (1994).
[22] P. J. Hajduk, D. A. Horita, and L. E. Lerner, J. Magn. Reson., Ser. A **103**, 40 (1993).
[23] D. E. Rourke, L. Khodarinova, and A. A. Karabanov, Phys. Rev. Lett. **92**, 163003 (2004).
[24] M. Lapert, Y. Zhang, M. Braun, S. J. Glaser, and D. Sugny, Phys. Rev. Lett. **104**, 083001 (2010).
[25] B. Bonnard and D. Sugny, SIAM J. Control Optim. **48**, 1289 (2009).
[26] B. Bonnard, M. Chyba, and D. Sugny, IEEE Trans. Autom. Control **54**, 2598 (2009).

[27] D. Sugny, C. Kontz, and H. R. Jauslin, Phys. Rev. A **76**, 023419 (2007).
[28] B. B. Laird and J. L. Skinner, J. Chem. Phys. **94**, 4405 (1991).
[29] H. M. Sevian and J. L. Skinner, J. Chem. Phys. **91**, 1775 (1989).
[30] A. A. Goun and B. Ya. Zel'dovich, J. Mod. Opt. **49**, 503 (2002).
[31] M. L. Aolita, I. Garcia-Mata, and M. Saraceno, Phys. Rev. A **70**, 062301 (2004); C. Altafini, J. Math. Phys. **44**, 2357 (2003).
[32] D. J. Tannor and A. Bartana, J. Phys. Chem. A **103**, 10359 (1999).
[33] M. Lapert, Y. Zhang, S. J. Glaser, and D. Sugny, J. Phys. B **44**, 154014 (2011).
[34] E. Assémat, M. Lapert, Y. Zhang, M. Braun, S. J. Glaser, and D. Sugny, Phys. Rev. A **82**, 013415 (2010).